DR. CHARLES F SCHULER IV (Orcid ID : 0000-0001-5656-7418)
DR. CATHERINE PTASCHINSKI (Orcid ID : 0000-0002-2098-8373)

Article type : Original Article: Asthma and Lower Airway Disease

Inhibition of uric acid or IL-1β ameliorates respiratory syncytial virus immunopathology and development of asthma

Running title: Uric acid or IL-1β inhibition ameliorates RSV and asthma

Charles F. Schuler IV, MD [1,3], Carrie-Anne Malinczak, BS [2], Shannon K. K. Best [2], Susan B. Morris, BS [2], Andrew J. Rasky, BS [2], Catherine Ptaschinski, PhD [2,3], Nicholas W. Lukacs, PhD [2,3], and Wendy Fonseca, DVM, PhD [2]

[1]Division of Allergy and Clinical Immunology, Department of Internal Medicine, [2]Department of Pathology, [3]Mary H. Weiser Food Allergy Center, University of Michigan, Ann Arbor, MI, USA, 48109.

Corresponding Authors:
Charles Schuler
Address: Domino's Farms, 24 Frank Lloyd Wright Drive, Suite H-2100, Ann Arbor, MI 48106.
Phone: 734-647-5940. Fax 734-647-6263. Email: schulerc@med.umich.edu.
Wendy Fonseca
Address: 109 Zina Pitcher Place / 4668 BSRB, Ann Arbor, MI 48109. Phone: 734-615-2544
Email: wfaguila@med.umich.edu

Abstract

Background: Respiratory Syncytial Virus (RSV) affects most infants early in life and is associated with increased asthma risk. The specific mechanism remains unknown.

Objective: To investigate the role of uric acid (UA) and IL-1β in RSV immunopathology and asthma predisposition.

Methods: Tracheal aspirates from human infants with and without RSV were collected and analyzed for pro-IL-1β mRNA and protein to establish a correlation in human disease. Neonatal mouse models of RSV were employed, wherein mice infected at 6-7 days of life were analyzed at 8 days post-infection, 5 weeks post-infection, or after a chronic cockroach allergen asthma model. A xanthine oxidase inhibitor or IL-1 receptor antagonist was administered during RSV infection.

Results: Human tracheal aspirates from RSV-infected infants showed elevated pro-IL-1β mRNA and protein. Inhibition of UA or IL-1β during neonatal murine RSV infection decreased mucus production, reduced cellular infiltrates to the lung (especially ILC2s), and decreased type 2 immune responses. Inhibition of either UA or IL-1β during RSV infection led to chronic reductions in pulmonary immune cell composition and reduced type 2 immune responses and reduced similar responses after challenge with cockroach antigen.

Conclusions: Inhibiting UA and IL-1β during RSV infection ameliorates RSV immunopathology, reduces the consequences of allergen-induced asthma, and presents new therapeutic targets to reduce early-life viral-induced asthma development.

Key Words: Respiratory syncytial virus, uric acid, xanthine oxidase, xanthine oxidase inhibitor, allopurinol, interleukin-1 beta, interleukin-1 receptor antagonist, Anakinra, asthma

Abbreviations:

Uric Acid: UA

IL-1 receptor antagonist: IL-1RA

Respiratory syncytial virus: RSV

Cockroach antigen: CRA

Type 2 innate lymphoid cells: ILC2(s)

Xanthine oxidase inhibitor: XOI

Interleukin: IL

Institutional Animal Care & Use Committee: IACUC

Plaque forming units: PFU
Protein nitrogen units: PNU
Lung draining lymph nodes: LDLN
Multiplicity of infection: MOI
Standard error of the mean: SEM
Periodic acid Schiff: PAS
Hematoxylin and eosin: H/E
Interferon: IFN
T helper cell type: Th
Bronchoalveolar Lavage: BAL

Disclosures: Dr. Schuler has nothing to disclose. Dr. Malinczak has nothing to disclose. Ms. Best has nothing to disclose. Mr. Rasky has nothing to disclose. Ms. Morris has nothing to disclose. Dr. Ptaschinski has nothing to disclose. Dr. Lukacs reports grants from the NIH during the conduct of the study. Dr. Fonseca has nothing to disclose.

Acknowledgements:
The manuscript was supported in part by NIH grants 5T32HL007517-30 (NWL), PO1AI1089473 (NWL), and AI138348 (NWL).

Author Contributions: The experiments were designed by C.F.S, N.W.L., and W.F. Experiments were performed by C.F.S., C.A.M., S.K.B., S.B.M., A.J.R., C.P. and W.F. Manuscript was written by C.F.S., N.W.L. and W.F. Data analysis was performed by C.F.S., N.W.L., and W.F. All authors participated in editing the manuscript.

Introduction

Respiratory syncytial virus (RSV) can cause bronchiolitis and affects most infants before age two [1, 2]. The global health burden of RSV includes over three million hospitalizations and ~100,000 deaths yearly among children under age five [3]. Severe RSV with bronchiolitis requiring hospitalization in infants is associated with an increased risk of childhood asthma [4-6]. RSV bronchiolitis involves airway epithelial loss, mucus over-production, pulmonary inflammatory infiltrates, and pulmonary obstruction [7, 8]. Severe RSV

infection involves excessive Th2 and Th17 immune responses [9-13]. These responses persist even after viral clearance and are associated with enhanced type 2 immune responses in models of asthma induced later in life [14]. Type 2 innate lymphoid cells (ILC2s) are an important source of IL-13, which is associated with mucus production and goblet cell hyperplasia in the lung [15-17]. RSV induces IL-13-producing ILC2 accumulation, which is associated with disease severity [7]. IL-1β, a regulator of ILC2s [18], has been described to be increased during RSV infection and may be directly involved in the pathogenesis [19, 20].

The precise connections between RSV induction of IL-1β, ILC2 activation, and RSV immunopathology remain unexplored. Uric acid production can induce reactive oxygen species production and thus activate the NLRP3 inflammasome, leading to IL-1β liberation [21-23] Inflammasome-activating metabolic products including uric acid (UA) are associated with IL-1β production and subsequent childhood wheezing or bronchitis [24]. In this work, we investigate the roles of UA and IL-1β during neonatal RSV infection using human samples and mouse models. We demonstrate that interrupting the uric acid pathway using a xanthine oxidase inhibitor (XOI) or blocking the downstream inflammation with an IL-1 receptor antagonist (IL-1RA) can ameliorate RSV immunopathology. The protective effects of the XOI or IL-1RA during RSV persist and are each protective from subsequent cockroach allergen (CRA) induction of asthma exacerbation.

Materials and Methods

Animals

The Institutional Animal Care & Use Committee (IACUC), University of Michigan, Ann Arbor, approved all animal use protocols, and all experiments proceeded according to IACUC guidelines. BALB/c mice 6-8 weeks old were purchased from Jackson Laboratory (Bar Harbor, ME). These were bred 1:1 male:female to produce neonates. Each individual litter underwent a single, uniform treatment condition, and the multiple litters undergoing different treatment conditions were treated on the same dates. Treatment conditions were replicated across multiple mouse cohorts. Standard pathogen-free conditions were maintained in the Unit for Laboratory Animal Medicine at the University of Michigan.

Patient Samples

All human studies were performed in accordance with an approved University of Michigan institutional review board protocol. Tracheal aspirate samples were obtained from

RSV-infected infants hospitalized and mechanically ventilated in a pediatric intensive care unit; baseline clinical characteristics were collected from the medical record and are summarized in supplemental table 1. Infants' parents or legal guardians provided informed consent. The samples were directly aspirated from the endotracheal tube. RSV infection was detected by clinical sputum PCR for initial diagnosis; this was confirmed subsequently by PCR in the lab (see below). Infants intubated for other non-infectious reasons provided control samples. Samples were divided for protein and cDNA analysis. Protein samples were diluted 1:1 with PBS-containing complete anti-protease cocktail (Sigma-Aldrich, St. Louis, MO) and 0.5% Triton X-100 nonionic detergent to dissociate mucus. TRIzol reagent was used for RNA extraction (Invitrogen, Carlsbad, CA). cDNA was synthesized using a murine leukemia virus reverse transcriptase (Applied Biosystems, Foster City, CA). Pro-IL-1β mRNA was analyzed via commercial Taqman primers (Thermo Fisher Scientific, Waltham, MA). IL-1β and CCL5 protein were measured using a Bio-Plex 200 System (Bio-Rad Laboratories, Hercules, CA).

RSV

RSV line 19, subgroup A, isolated from an infected infant at the University of Michigan Children's Hospital, was used for all experiments as previously described [25]. We have previously demonstrated animal models with this virus mimic human RSV with mucus hypersecretion and cytokine dysregulation [26]. Neonatal animals were infected with 1.8×10^5 plaque forming units (PFU) via intranasal instillation.

Primary RSV Infection Time-course

Neonatal BALB/c mice were infected with RSV at 6-7 days old. Mice were sacrificed at day 2, 4, 6, 8, and 14 post-infection. Control mice were sham infected with carrier fluid. Separate age-matched control groups were used at each time-point. Lungs were flash frozen for RNA evaluation. BAL was collected as below.

Primary RSV Infection

BALB/c mice were infected with RSV at 6-7 days old. Mice were treated daily with the relevant inhibitor starting on the day of infection for seven days. At 4, 6, or 8 days post-infection the mice were sacrificed. Whole lungs and lung draining lymph nodes (LDLN) were isolated for flow cytometry, histology, PCR, and/or cytokine analysis (Supplemental Fig. 1). Control RSV-infected animals were treated with carrier fluid in these experiments. For

experiments where the XOI and IL-1RA groups were both included, the IP carrier fluid-treated, RSV-infected control group was used.

Xanthine Oxidase Inhibitor Treatment

The XOI, allopurinol, (Sigma Aldrich, St. Louis, MO) was administered at 25 μg per mouse (approximately 10 mg/kg) via intraperitoneal injection (volume 50 μL) daily starting on the day of RSV infection for seven doses. The dose was chosen based on prior dose-finding experiments (internal data) and known human dosing for allopurinol in children [27-29].

Interleukin-1 Receptor Antagonist

The IL-1RA (Cayman Chemical, Ann Arbor, MI) was administered daily at 0.2 μg per mouse (approximately 0.08 mg/kg) via intranasal instillation (volume 5 μL) starting on the day of RSV infection for seven doses. This dose was chosen based on prior dose-finding experiments that suggested this dose was safe and potentially effective.

Chronic RSV Model

BALB/c mice were infected with RSV at day 6-7 of life. The mice were treated daily with either XOI or IL-1RA as above. After seven daily treatments the mice rested four weeks. RSV-infected controls were treated with carrier fluid. The mice were euthanized, and whole lungs and LDLN were isolated for flow cytometry, histology, PCR, and/or cytokine analysis (Supplemental Fig. 1A).

Cockroach antigen (CRA) model

BALB/c mice were infected with RSV as above at 6-7 days old. The mice were treated daily with either inhibitor as above. After seven treatments the mice rested four additional weeks. The mice then began CRA sensitization and challenge as previously described [14, 30, 31]. Briefly, mice were sensitized with 500 protein nitrogen units (PNU) of CRA on days 0, 1, 2 and challenged with 500 PNU on days 14, 20, 22, and 23. The CRA was clinical grade used for skin testing (Hollister-Stier, Spokane, WA). On day 24, the mice were sacrificed, and whole lungs and LDLN were isolated for flow cytometry, histology, PCR, and/or cytokine analysis (Supplemental Fig. 1B).

Flow Cytometry

Lungs were enzymatically dispersed with collagenase A 1 mg/mL (Roche, Indianapolis, IN) and 20 U/mL DNase I (Sigma, St. Louis, MO) in RPMI with 10% FCS and further dispersed via 18-gauge needle (10 mL syringe). RBCs were lysed and samples

filtered through 100-micron nylon mesh. Cells were re-suspended in PBS. LIVE/DEAD stain kit identified live cells (Thermo Fisher Scientific, Waltham, MA). Cells were washed and re-suspended in PBS with 1% FCS. Fc receptors were blocked with anti-CD16/32 (BioLegend, San Diego, CA). Surface markers were identified using the following clonal antibodies, all from BioLegend: anti-Gr-1 (RB6- 8C5), B220 (RA3-6B2), CD3 (145-2C11), Ter119 (Ter-119), CD11b (M1/70), CD25 (PC61), CD45 (30-F11), ST2 (DIH9), c-Kit (2B8), CD90 (53-2.1), CD4 (RM4-5), CD3 (17A2), CD8 (53-5.8), CD69 (H1.2F3) CD11c (N418), MHCII (M5/114.15.2), CD103 (2E7). SiglecF was from BD Biosciences (San Jose, CA). For innate lymphoid staining, anti-CD3, CD11b, B220, Gr-1, TER119, and GATA3 were used (eBioscience/Thermo Fisher) in accordance with a previously published protocol [32]. For ILC2: Lin-(CD3, CD11b, B220, GR-1, TER119) CD45+CD25+CD90+ST2+c-Kit+ +GATA3+. For eosinophils: SSC^{high}CD11b+SiglecF+. For neutrophils: SSC^{high}CD11b+SiglecF-GR-1+. For conventional DC: CD11b+CD11c+MHCII+, CD103-. For DC 103+: CD11c+ CD11b-MHCII+CD103+. For interstitial macrophages: CD11b+CD11c-F4/80+. For T cells CD4+: CD3+CD4+, T cells CD8+: CD3+CD8+. Data were collected using a NovoCyte flow cytometer (ACEA Bioscience, San Diego, CA), and analysis utilized FlowJo software (Tree Star, OR). Gating strategies are available in the Supplementary Data (supplemental figure 4).

Histology

The middle and inferior lobes of the right lung were perfused with formaldehyde and embedded in paraffin. Five-micron lung sections were stained with periodic acid-Schiff (PAS) or hematoxylin/eosin (H/E). A Zeiss Axio Imager Z1 with AxioVision 4.8 software (Zeiss, Munich, Germany) collected photomicrographs.

Mucus Scoring Analysis

Slides from PAS-stained lungs were coded and scored by a blinded observer. Mucus was quantified on a score of 1-4, with 1 = minimal/no mucus; 2 = slight: multiple airways with goblet cell hyperplasia and mucus; 3 = moderate: multiple airways with significant mucus and some plugging; 4 = severe: significant mucus plugging [14].

Quantitative RT-PCR

TRIzol reagent was used for lung tissue homogenization and RNA extraction (Invitrogen, Carlsbad, CA). cDNA was synthesized using murine leukemia virus reverse transcriptase (Applied Biosystems, Foster City, CA) incubated at 37 ℃ followed by 95 ℃ to

stop the reaction. Real-time quantitative PCR (qPCR) using Taqman (Thermo Fisher Scientific, Waltham, MA) primers with a FAM-conjugated probe measured pro-IL-1β (Mm00434228 and Hs01555410), IL-4 (Mm00445259), IL-5 (Mm00439646), IL-13 (Mm00434204), CCL5 (Mm01302428), xanthine oxidase (Mm00442110), interferon-γ (Mm00801778), and 18S (Hs99999901 and Mm03928990). A previously described primer system was used to measure Gob5 [33]. Custom primers were used for RSV-G (forward: CCA AGC AAA CCC AAT AAT GAT TT, reverse: GCC CAG CAG GTT GGA TTG T) (Sigma Aldrich, St. Louis, MO). Gene expression was normalized to 18S expression with fold-change values calculated using $2^{-\Delta\Delta}$ cycle threshold method relative to uninfected wild-type controls. For the human pro-IL-1β expression, human 18S expression was used for normalization. A 7500 Real-Time PCR System (Applied Biosystems, Foster City, CA) was used.

Re-stimulation of Lung-Draining Lymph Node (LDLN) Cells with RSV or CRA

LDLN were digested via 1 mg/mL collagenase A (Roche) and 25 U/mL DNase I (Sigma Aldrich) in RPMI with 10% FCS for 45-60 minutes at 37°C and further dispersed via 18-gauge needle (10 mL syringe). RBCs were lysed and samples filtered through 100-micron nylon mesh. Single-cell suspensions of lymph nodes at a concentration of 2.5 x 10^6 cells/mL (0.2 mL plated per well) in a 96 well plate were re-stimulated with RSV 5 x 10^5 PFU or CRA 300 PNU as appropriate. The supernatants were collected at 48 hours and analyzed for the following cytokines: IFN-γ, IL-4, IL-5, and IL-13 using a Bio-Plex bead-based cytokine assay (Bio-Rad Laboratories, Hercules, CA).

Bronchoalveolar Lavage

Bronchoalveolar lavage (BAL) was performed on neonatal mice after euthanasia. The trachea and lungs in the neck and chest were directly exposed. A 26 gauge needle was inserted into the trachea and 200 uL of PBS was instilled gently, and the lungs were directly visualized to inflate. Approximately 100 uL was returned upon application of suction. This was frozen at -20°C until analysis.

Lung Extracts

The left lung was taken for protein measurement. Each lung was placed in Tissue Protein Extraction Reagent (Thermo Fisher) 1 mL and total protein was extracted according to the manufacturer's protocol. This was frozen at -20°C until analysis.

Uric Acid Measurements

BAL samples taken from neonatal mice at 6 days post-infection after euthanasia were analyzed for uric acid content. The uric acid assay kit (Cayman Chemicals, Ann Arbor, MI) using the manufacturer's instructions was used.

Enzyme-Linked Immunosorbent Assays

Murine IL-1β protein was quantified from lung extract samples taken from naïve or infected mice at 6 days post-infection after euthanasia. We used the R&D Duo set ELISA kit (R&D Systems, Minneapolis, MN) and followed the manufacturer's instruction.

Statistical Analysis

Prism 7 (GraphPad Software) was used for data analysis. Data are presented as mean values +/- SEM. Unpaired, two-tailed t-test was used to compare data with two groups. ANOVA was used to compare three or more groups. A p-value < 0.05 was considered statistically significant.

Results

RSV induces pulmonary IL-1β expression in infants and neonatal mice.

In this work, we initially analyzed tracheal aspirates from human infants with severe RSV for the presence of IL-1β. We detected significantly increased mRNA expression of pro-IL-1β and protein production of IL-1β in the samples of RSV+ infants compared with controls (Fig. 1A and 1B). Protein production of CCL5, a chemokine known to be correlated with severe RSV disease [34], was also significantly elevated in samples from RSV-infected infants (Fig. 1C). IL-1β is known to be a potent cytokine that amplifies the immune response through the activation of cytokine cascades as well as activation of critical innate immune cells, such as ILC2s [18, 19, 35, 36]. Therefore, we decided to investigate the impact of IL-1β-induced immune activation on type 2 immunity-associated RSV immunopathology.

To study the role of IL-1β during RSV infection, a neonatal murine model was utilized to recapitulate responses in clinical disease in infants (Supplemental Fig. 1A) [14, 37]. To compare this model to the above human samples, neonatal BALB/c mice were infected with RSV line 19 and we measured mRNA expression of pro-IL1β and CCL5 in the lung. We observed significant increases in mRNA expression of both cytokines (Fig. 1D), resembling the RSV infection in infants. Various metabolic mediators have been identified to drive IL-1 pathway activation [23, 36], and RSV has been shown to alter metabolic profiles in mice as a key step driving immunopathology [38]. Examination of a key metabolic activator of IL-1β, uric

acid (UA), was performed by analyzing the expression of xanthine oxidase that converts xanthine to UA. A time-course of xanthine oxidase (XO) in the lungs of neonatal mice revealed high expression that peaked at 4 days post-infection (dpi) (Fig. 1D). RSV infection was confirmed in the model via PCR, with RSV-G peaking on day 4 post-infection (Supplemental Fig. 1C). Bronchoalveolar lavage (BAL) fluid taken from neonatal mice at 8 days post-infection demonstrated elevated levels of UA in RSV-infected mice compared to controls (Fig. 1E). Thus, we observed contemporaneous increased expression of XO, increased production of UA, and increased production of pro-IL-1β during neonatal RSV infection.

Inhibition of uric acid or IL-1β pathway ameliorates RSV immunopathology.

To examine the role of the XOI or IL-1RA on RSV immunopathology, neonatal BALB/c mice infected with RSV were treated daily with either the xanthine oxidase inhibitor (XOI) or interleukin 1 receptor antagonist (IL-1RA) (Supplemental Fig. 1A). Examination of the histopathology demonstrated that the XOI treatment in particular reduced mucus production and goblet cell metaplasia compared with infected controls as well as an overall decrease in cellular infiltrates in the treated groups (Fig. 2A, 2B). We also observed downregulation of the mucous-associated gene Gob5 and the chemokine CCL5 in both treated groups (Fig. 2C). We evaluated viral clearance rates associated with the treatments using RSV-G RNA expression. No difference between control mice and XOI-treated mice was observed at day 4 of infection (Supplemental Fig. 1D). However, uric acid levels in BAL at day 6 post-infection were lower in XOI-treated animals compared to control mice (Fig. 2D). Local lung IL-1β levels were not significantly changed in XOI- or IL-1RA-treated animals at 4 days post infection (dpi) (Supplemental Fig. 1E). These data suggest that UA and IL-1β have important roles during RSV pathogenesis.

To characterize the immune response in neonatal mice infected with RSV that were treated with either XOI or IL-1RA, we analyzed pulmonary leukocyte populations by flow cytometry. During RSV infection, increased numbers of activated ILC2s have been reported [39]. In the present studies, ILC2 (Fig. 3A) and neutrophils (Fig. 3B) were significantly increased in RSV infection and reduced in both XOI- or IL-1RA-treated mice compared with infected controls. Other leukocytes including macrophages, CD4+ T cells, eosinophils, and dendritic cell populations were not significantly altered by RSV infection at this time-point

(Supplemental Fig. 1F, 1G, 1H, 1I, 1J). To further evaluate the immune response, we measured cytokine levels from isolated lung draining lymph node (LDLN) cells after *in vitro* re-stimulation with RSV and observed that the XOI-treated neonatal group had reduced IL-4, IL-5, and IL-13 production (Fig. 3C, 3D, 3E) and increased IFN-γ and IL-17A production (Fig. 3F, Supplemental Fig. 3A) compared to RSV-infected control animals. The IL-1RA-treated group also demonstrated reduced IL-4 production (Fig. 3C), but no change in IL-5 or IL-13 (Fig. 3D, 3E), and an increase in IFN-γ and IL-17A levels compared to the control group (Fig. 3F, Supplemental Fig. 3A). Altogether, both XOI and IL-1RA treatment reduce type 2 immune responses during RSV infection and promote a type 1 immune response.

Control of RSV disease severity by XOI or IL-1RA treatments establish long-lasting immune changes.

To evaluate long-term consequences of XOI or IL-1RA treatment during RSV infection, neonatal mice were infected at day 6-7 of life and treated with the XOI or IL-1RA daily for 7 days. At five weeks after infection the lungs were evaluated for their mucus expression and immune phenotype. No significant differences were observed between naïve animals, RSV-infected mice, or either treated group in visible lung pathology by PAS staining or in mucus gene expression by qPCR (Supplemental figure 2A, 2B, 2C). However, there was a persistent increase in ILC2s in the lungs of RSV-infected mice, that was significantly reduced in the groups of mice that were treated with XOI or IL-1RA (Fig 4A). In addition, increased macrophage, CD103+ dendritic cell, and eosinophil numbers were decreased in the IL-1RA-treated group, while only a non-significant trend toward reduction in these cell types in the XOI-treated group (Fig. 4B, 4C, 4D). CD4+ T cell and neutrophil numbers were unchanged in the treated groups (Supplemental figure 2D). To evaluate the lymphocyte responses to RSV re-stimulation, LDLN were harvested from animals infected with RSV with XOI or IL-1RA treatment and compared to infected controls. The XOI-treated mice showed an increase in IL-4 production (Fig. 4E), no change in IL-5 (Fig. 4F), and a significant decrease in IL-13 production (Fig 4G) compared to RSV-infected mice. The IL-1RA-treated group showed significant reduced production of IL-4, IL-5, and IL-13 (Fig. 4E, 4F, 4G). Both treated groups showed a decrease in IFN-γ and no change in IL-17A production (Fig. 4H, Supplemental Fig. 3B). Thus, there appears to be persistent innate immune cells in the lung and altered immune

responses long after RSV infection has cleared that are attenuated in the XOI- or IL-RA-treated animals.

Control of RSV infection severity by XOI or IL-1RA treatments ameliorates exacerbated development of asthma.

In order to evaluate whether the changes with XOI or IL-1RA treatment during RSV infection would affect subsequent asthma development, RSV-infected mice were exposed to an allergen challenge model of asthma. Five-week-old mice previously infected with RSV and treated with XOI or IL-1RA were sensitized and challenged with cockroach antigen (CRA) (Supplemental Fig. 1B). Lung histology demonstrated a decrease in mucus deposition (Fig. 5A) and less prominent inflammatory leukocyte infiltrates in the group of mice treated with XOI or IL-1RA compared to untreated animals during the neonatal RSV infection (Fig. 5B). Mucus scoring was lower in the treated animal groups as well (Fig. 5C). Gob5 mucus-related gene expression in the lung was reduced in XOI- and IL-1RA-treated animals (Fig. 5D). CRA treatment increased IL-13 gene expression in the lung and the enhanced IL-13 was decreased in the IL-1RA-treated group (Fig. 5E).

To investigate the effect of blocking the XO and IL-1β pathways during RSV infection on the lung immune environment, flow cytometry was performed in the asthma model. Interestingly, the XOI- or IL-1RA-treated mice demonstrated no change in ILC2 numbers during CRA challenge when compared to RSV-infected/CRA-treated controls (RSV/CRA) (Fig. 6A). However, reduced numbers of interstitial macrophages in the lung of the XOI- or IL-1RA-treated mice were observed (Fig. 6B). Although there were no significant differences in the CD4+ T cells or CD103+ dendritic cells in either of the treated groups (Fig. 6C, 6F), there was a significant reduction in eosinophils and CD11b+ dendritic cells in IL-1RA-treated mice (Fig. 6D, 6E). Thus, differences in the cellular infiltrate changes in the XOI or IL-1RA treated groups lead to reductions in pulmonary immune infiltrates during subsequent induction of asthmatic disease.

Finally, we evaluated the acquired immune response by *in vitro* re-stimulation of LDLN from asthmatic mice with allergen. The groups treated with XOI and IL-1RA during neonatal RSV infection both demonstrated reduced IL-4, IL-5, and IL-13 production upon CRA re-stimulation (Fig. 6G, 6H, 6I), with no change in IL-17A production (Supplemental Fig. 3C), and the IL-1RA group also showed reduced IFN-γ (Fig. 6J). These data suggest that type 2

immunity induced in the RSV/CRA model is reduced by XOI or IL-1RA treatment during neonatal RSV infection. Together, these data indicate that control of neonatal RSV immunopathology, by XOI or IL-1RA treatment translates into long term control of type 2 immune responses in the lung upon later allergen sensitization and attenuates the RSV-associated asthma predisposition.

Discussion

In this work we demonstrated that inhibition of the uric acid or IL-1β pathways by the XOI (allopurinol) or IL-1RA (Anakinra) treatments in RSV-infected neonatal mice decreased RSV immunopathology and ameliorated the long-term type 2 immunity-associated asthma exacerbation. Given the high global health burden of RSV, with over three million hospitalizations and ~100,000 deaths worldwide yearly among children under age five, disrupting the immunopathology of early life-RSV infection with allopurinol or Anakinra could directly have a significant impact on health. In addition, because early life viral infections, especially RSV, are associated with development of asthma, these treatments might lead to long-term reductions in childhood asthma. Prior work has shown the important role of metabolic alterations in RSV immunopathology [38]. Thus, these studies provide novel and striking evidence that interrupting this metabolic and inflammatory process could have significant clinical impact.

Uric acid is a product of purine metabolism produced by xanthine oxidase [40] and is produced during cell injury with viral infections [41]. UA has been implicated in house dust mite pulmonary injury and as an adjuvant promoting asthma; allopurinol can disrupt UA's deleterious effects [40, 42-44]. Allopurinol is well-studied with a long-standing safety record [45] and has been used for many years in diseases such as gout to normalize the level of system UA to reduce flares [46, 47]. In addition, dosing and safety data are available in children, particularly with treating tumor lysis syndrome [27-29]. This process of blocking UA production may be especially viable in disease such as viral infections that promote high levels of production since humans do not produce uricase to further process UA [48]. Thus, while further clinical research will be needed, safety and dosing has already been established in children and infants making this a potential clinical option to add to the clinical "tool-box".

IL-1β is a major inflammasome output, which can be activated by UA through the NLRP3 pathway [23, 36]. IL-1β is elevated in nasopharyngeal aspirates of infants with RSV,

and in murine models plays a role in RSV immunopathology [19, 49, 50], and a role for NLRP3-inflammasome activation of IL-1β has been shown in models of rhinovirus [51]. IL-1β promotes type 2 immune responses in asthma, IL-1β is upregulated in BAL fluid from Th2/Th17 polarized asthmatic patients, IL-1β elevation is associated with increased rates of hospitalization in asthmatic patients, and murine asthma models demonstrate a role for IL-1β in regulating barrier function and mucin production [20, 52-54]. While we suspect that the IL-1RA affects IL-1β signaling through the IL-1 receptor, we acknowledge that these data do not definitively prove this connection; future studies are needed to understand this mechanism fully.

Like allopurinol, there are established safety and dosing profiles for IL-1RAs in children [55-57]. IL-1RAs, particularly Anakinra, are widely used in juvenile rheumatoid arthritis to reduce IL-1-related inflammation [55-57]. Furthermore, IL-1RAs are effectively and safely deployed in various autoinflammatory syndromes, including cryopyrin-associated periodic fever syndromes, tumor necrosis factor-associated periodic fever syndromes, familial Mediterranean fever, and adult-onset Stills disease [58-61]. However, IL-1RAs have not been evaluated as a therapy for RSV to potentially reduce asthma.

There are differences in the outcome of disease phenotypes between the XOI and IL-1RA treatments in this study. These differences are likely because UA can affect multiple pathways including inflammasome activation, while IL-1β may have a more targeted and specific effect on the downstream inflammation. In this case, the lack of decrease in IL-1β during RSV infection with XOI-treatment suggests IL-1 independent pathways may play a role. Allopurinol appears to provide a more robust reduction in RSV immunopathology acutely than the IL-1RA, whereas the IL-1RA effects are more persistent when examining pulmonary infiltrates and LDLN at later time points, despite the slightly higher viral levels seen in the acute infection. Further, CD103+ dendritic cells were reduced in the IL-1RA-treated mice in the later allergen model in the IL-1RA treatment, which corresponded with a reduction in IFN-γ on LDLN re-stimulation consistent with prior work [62, 63]. Both inhibitors lead to marked reductions in ILC2s, which can play a role in RSV immunopathology and type 2 immune responses [39]. Given the perceived ability of ILC2s to establish an allergic immune environment in the lung [64], this modified phenotype may be desirable and play a key role. The differences extend to the later development of allergic disease, where the IL-1RA-treated

mice demonstrate greater reductions in pulmonary IL-13 expression, pulmonary cellular infiltrates, and type 2 immune responses in LDLN lymphocytes than XOI-treated animals. However, since both treatments reduce the overall disease the use of them individually or together may be a clinical decision based upon the viral induced phenotype and severity presented in each infant. These differences may depend upon, for example, the level of UA vs. IL-1β in airway samples or the metabolic state of the infected patient.

This novel work verifies and connects the metabolic consequences and immunopathology of RSV infection. We propose a conceptual model (see graphical abstract) to explain how these two processes might be linked. We show that UA production is induced by RSV infection, and that this activates the inflammasome, leading to IL-1β production. IL-1β, known to induce ILC2 activation and proliferation, likely promotes a type 2 immune environment coupled with persistent changes in the airway, such as goblet cell metaplasia. By inhibiting either xanthine oxidase or the IL-1 receptor, we can interrupt this process, with beneficial immediate and long-term consequences. This neonatal murine model reflects the time in life that this infection has the most consequences in humans [2]. However, since the clinical burden of RSV is not limited to infants, these treatments could have impacts on RSV infection in the elderly as well as those with chronic lung disease, such as COPD [65-67]. This work extends to development of asthma early in life, which may be a clinical consequence of RSV infection, and these inhibitors may attenuate subsequent asthma. Further research, pre-clinical and clinical, could provide better definitions of how and when to use specific inhibitors during disease.

Figure Legends

Figure 1. RSV induces pulmonary IL-1β expression in humans and mice neonates.
A) cDNA from tracheal aspirates from human infants with RSV and from control patients intubated for non-infectious reasons underwent qPCR to determine pro-IL-1β mRNA (N ≥ 9). B) Tracheal aspirates from human infants underwent Bioplex to determine IL-1β protein concentration (N ≥ 6). C) Tracheal aspirates from human infants were measured via Bioplex to determine CCL5 protein concentration (N ≥ 7). D) Mice infected with RSV were sacrificed at 2, 4, 8, and 14 days post-infection (dpi) and compared with age-matched controls. Lungs were homogenized and mRNA extracted to determine CCL5, pro-IL-1β, and xanthine oxidase

mRNA expression (N ≥ 5). E) BAL fluid from mice with RSV and age-matched controls was taken 8 days post-infection and assayed for uric acid (N ≥ 6). Data represent mean +/- SEM. *p < 0.05, **p < 0.01.

Figure 2. Administration of the XOI or IL-1RA ameliorates RSV infection.

Mice were infected with RSV and treated with the XOI or IL-1RA and compared with infected mice at 6 or 8 days post infection. A) Lungs were embedded in paraffin and Periodic acid-Schiff (PAS) stained to visualize mucous (pink/purple staining) or hematoxylin/eosin (H/E) stained to evaluate inflammatory cell infiltrates. Representative photos shown (N ≥ 5). B) Mucus scoring was performed on blinded histological slides on a scale of 1–4 for mucus production (N ≥ 4). C) Lungs were homogenized and mRNA extracted to determine Gob5 mRNA expression (N ≥ 5) and CCL5 mRNA expression (N ≥ 6). D) BAL fluid at 6 days post-infection was collected as described and assayed for uric acid content (N ≥ 4). Data represent mean +/- SEM. *p < 0.05. **p < 0.01, ***p < 0.001.

Figure 3. Administration of the XOI or IL-1RA reduces pulmonary immune infiltrates and lymphocyte responsiveness with RSV infection.

Mice were infected with RSV and treated with the XOI or IL-1RA and compared with infected mice at 8 days post-infection. A and B) Lungs were processed into single-cell suspension, then stained and analyzed via flow cytometry for type 2 innate lymphoid cells (N ≥ 6) and neutrophils (N ≥ 5). C, D, E, and F) Lung draining lymph nodes were processed into single-cell suspension and re-stimulated with RSV *in vitro* for 48 hours to determine cytokine protein levels in the supernatant including IL-4, IL-5, IL-13, and IFN-γ (N ≥ 3). Data represent mean +/- SEM. *p < 0.05, **p < 0.01, ***p < 0.001, ****p < 0.0001.

Figure 4. Administration of the XOI or IL-1RA during RSV infection leads to durable immune changes.

Mice were infected with RSV and treated with the XOI or IL-1RA and compared with infected mice at 5 weeks' post infection. A, B, C, D) Lungs were processed into single-cell suspensions, then stained and analyzed via flow cytometry for type 2 innate lymphoid cells,

macrophages, CD103+ dendritic cells, and eosinophils (N ≥ 4). E, F, G, and H) Lung draining lymph nodes were processed into single-cell suspension and re-stimulated with RSV *in vitro* for 48 hours to determine cytokine protein levels in the supernatant including IL-4, IL-5, IL-13, and IFN-γ (N ≥ 6). Data represent mean +/- SEM. *p < 0.05, **p < 0.01, ***p < 0.001, ****p < 0.0001.

Figure 5. Administration of the XOI or IL-1 receptor antagonist during RSV infection ameliorates lung immunopathology during subsequent cockroach antigen sensitization.

Mice were infected with RSV and treated with the XOI or IL-1RA. 5 weeks after the start of infection, mice underwent CRA sensitization and challenge. Control mice were uninfected, CRA-treated mice (CRA only), and RSV-infected/CRA-treated mice (RSV/CRA). A and B) Lungs were embedded in paraffin and Periodic acid-Schiff (PAS) stained to visualize mucous (pink/purple staining) or hematoxylin/eosin (H/E) stained to evaluate inflammatory cell infiltrates. Representative photos shown (N ≥ 9). C) Mucus scoring was performed on blinded histological slides on a scale of 1–4 for mucus production (N ≥ 9). D and E) Lungs were homogenized and mRNA extracted to determine Gob5 (N ≥ 8) and IL-13 mRNA expression (N ≥ 3). Data represent mean +/- SEM. *p < 0.05, **p < 0.01.

Figure 6. Administration of the XOI or IL-1 receptor antagonist during RSV infection ameliorates type 2 immune responses during subsequent cockroach antigen sensitization.

Mice were infected with RSV and treated with the XOI or IL-1RA. 5 weeks after the start of infection, mice underwent CRA sensitization and challenge. Control mice were uninfected, CRA-treated mice (CRA only) as well as RSV-infected/CRA-treated mice (RSV/CRA). A, B, C, D, E, F) Lungs were processed into single-cell suspensions, then stained and analyzed via flow cytometry for type 2 innate lymphoid cells (N ≥ 7), macrophages (N ≥ 8), CD4+ T cells (N ≥ 4), eosinophils (N ≥ 8), CD11b+ dendritic cells (N ≥ 8), and CD103+ dendritic cells (N ≥ 8). G, H, I, and J) Lung draining lymph nodes were processed into single-cell suspension and re-

stimulated with RSV *in vitro* for 48 hours to determine cytokine protein levels in the supernatant including IL-4, IL-5, IL-13, and IFN-γ (N ≥ 8). Data represent mean +/- SEM. *p < 0.05, **p < 0.01, ***p < 0.001, ****p < 0.0001.

References

1. Heilman, C.A., *From the National Institute of Allergy and Infectious Diseases and the World Health Organization. Respiratory syncytial and parainfluenza viruses.* J Infect Dis, 1990. **161**(3): p. 402-6.
2. Openshaw, P.J., G.S. Dean, and F.J. Culley, *Links between respiratory syncytial virus bronchiolitis and childhood asthma: clinical and research approaches.* Pediatr Infect Dis J, 2003. **22**(2 Suppl): p. S58-64; discussion S64-5.
3. Shi, T., et al., *Global, regional, and national disease burden estimates of acute lower respiratory infections due to respiratory syncytial virus in young children in 2015: a systematic review and modelling study.* Lancet, 2017. **390**(10098): p. 946-958.
4. Sigurs, N., et al., *Asthma and allergy patterns over 18 years after severe RSV bronchiolitis in the first year of life.* Thorax, 2010. **65**(12): p. 1045-52.
5. Henderson, J., et al., *Hospitalization for RSV bronchiolitis before 12 months of age and subsequent asthma, atopy and wheeze: a longitudinal birth cohort study.* Pediatr Allergy Immunol, 2005. **16**(5): p. 386-92.
6. Castro, M., et al., *Cytokine response after severe respiratory syncytial virus bronchiolitis in early life.* J Allergy Clin Immunol, 2008. **122**(4): p. 726-733 e3.
7. Stier, M.T., et al., *Respiratory syncytial virus infection activates IL-13-producing group 2 innate lymphoid cells through thymic stromal lymphopoietin.* J Allergy Clin Immunol, 2016. **138**(3): p. 814-824 e11.
8. Johnson, J.E., et al., *The histopathology of fatal untreated human respiratory syncytial virus infection.* Mod Pathol, 2007. **20**(1): p. 108-19.
9. Mukherjee, S., et al., *IL-17-induced pulmonary pathogenesis during respiratory viral infection and exacerbation of allergic disease.* Am J Pathol, 2011. **179**(1): p. 248-58.

10. Hashimoto, K., et al., *Respiratory syncytial virus infection in the absence of STAT 1 results in airway dysfunction, airway mucus, and augmented IL-17 levels.* J Allergy Clin Immunol, 2005. **116**(3): p. 550-7.
11. Stoppelenburg, A.J., et al., *Elevated Th17 response in infants undergoing respiratory viral infection.* Am J Pathol, 2014. **184**(5): p. 1274-9.
12. Lukacs, N.W., et al., *Respiratory virus-induced TLR7 activation controls IL-17-associated increased mucus via IL-23 regulation.* J Immunol, 2010. **185**(4): p. 2231-9.
13. Lotz, M.T. and R.S. Peebles, Jr., *Mechanisms of respiratory syncytial virus modulation of airway immune responses.* Curr Allergy Asthma Rep, 2012. **12**(5): p. 380-7.
14. Malinczak, C.A., et al., *Sex-associated TSLP-induced immune alterations following early-life RSV infection leads to enhanced allergic disease.* Mucosal Immunol, 2019.
15. Halim, T.Y., et al., *Lung natural helper cells are a critical source of Th2 cell-type cytokines in protease allergen-induced airway inflammation.* Immunity, 2012. **36**(3): p. 451-63.
16. Barlow, J.L., et al., *Innate IL-13-producing nuocytes arise during allergic lung inflammation and contribute to airways hyperreactivity.* J Allergy Clin Immunol, 2012. **129**(1): p. 191-8 e1-4.
17. Zhu, Z., et al., *Pulmonary expression of interleukin-13 causes inflammation, mucus hypersecretion, subepithelial fibrosis, physiologic abnormalities, and eotaxin production.* J Clin Invest, 1999. **103**(6): p. 779-88.
18. Ohne, Y., et al., *IL-1 is a critical regulator of group 2 innate lymphoid cell function and plasticity.* Nat Immunol, 2016. **17**(6): p. 646-55.
19. Owczarczyk, A.B., et al., *Sirtuin 1 Regulates Dendritic Cell Activation and Autophagy during Respiratory Syncytial Virus-Induced Immune Responses.* J Immunol, 2015. **195**(4): p. 1637-46.
20. Besnard, A.G., et al., *NLRP3 inflammasome is required in murine asthma in the absence of aluminum adjuvant.* Allergy, 2011. **66**(8): p. 1047-57.
21. Braga, T.T., et al., *Soluble Uric Acid Activates the NLRP3 Inflammasome.* Sci Rep, 2017. **7**: p. 39884.
22. Ives, A., et al., *Xanthine oxidoreductase regulates macrophage IL1beta secretion upon NLRP3 inflammasome activation.* Nat Commun, 2015. **6**: p. 6555.

23. Martinon, F., et al., *Gout-associated uric acid crystals activate the NALP3 inflammasome.* Nature, 2006. **440**(7081): p. 237-41.
24. Herberth, G., et al., *Endogenous metabolites and inflammasome activity in early childhood and links to respiratory diseases.* J Allergy Clin Immunol, 2015. **136**(2): p. 495-7.
25. Moore, M.L., et al., *A chimeric A2 strain of respiratory syncytial virus (RSV) with the fusion protein of RSV strain line 19 exhibits enhanced viral load, mucus, and airway dysfunction.* J Virol, 2009. **83**(9): p. 4185-94.
26. Lukacs, N.W., et al., *Differential immune responses and pulmonary pathophysiology are induced by two different strains of respiratory syncytial virus.* Am J Pathol, 2006. **169**(3): p. 977-86.
27. Cortes, J., et al., *Control of plasma uric acid in adults at risk for tumor Lysis syndrome: efficacy and safety of rasburicase alone and rasburicase followed by allopurinol compared with allopurinol alone--results of a multicenter phase III study.* J Clin Oncol, 2010. **28**(27): p. 4207-13.
28. Smalley, R.V., et al., *Allopurinol: intravenous use for prevention and treatment of hyperuricemia.* J Clin Oncol, 2000. **18**(8): p. 1758-63.
29. Goldman, S.C., et al., *A randomized comparison between rasburicase and allopurinol in children with lymphoma or leukemia at high risk for tumor lysis.* Blood, 2001. **97**(10): p. 2998-3003.
30. Campbell, E.M., et al., *Monocyte chemoattractant protein-1 mediates cockroach allergen-induced bronchial hyperreactivity in normal but not CCR2-/- mice: the role of mast cells.* J Immunol, 1999. **163**(4): p. 2160-7.
31. Jang, S., et al., *Respiratory syncytial virus infection modifies and accelerates pulmonary disease via DC activation and migration.* J Leukoc Biol, 2013. **94**(1): p. 5-15.
32. Ting, H.A., et al., *Notch ligand Delta-like 4 induces epigenetic regulation of Treg cell differentiation and function in viral infection.* Mucosal Immunol, 2018. **11**(5): p. 1524-1536.
33. Miller, A.L., et al., *CXCR2 regulates respiratory syncytial virus-induced airway hyperreactivity and mucus overproduction.* J Immunol, 2003. **170**(6): p. 3348-56.

34. John, A.E., A.A. Berlin, and N.W. Lukacs, *Respiratory syncytial virus-induced CCL5/RANTES contributes to exacerbation of allergic airway inflammation.* Eur J Immunol, 2003. **33**(6): p. 1677-85.
35. Bohmwald, K., et al., *Contribution of Cytokines to Tissue Damage During Human Respiratory Syncytial Virus Infection.* Front Immunol, 2019. **10**: p. 452.
36. Im, H. and A.J. Ammit, *The NLRP3 inflammasome: role in airway inflammation.* Clin Exp Allergy, 2014. **44**(2): p. 160-72.
37. Cormier, S.A., D. You, and S. Honnegowda, *The use of a neonatal mouse model to study respiratory syncytial virus infections.* Expert Rev Anti Infect Ther, 2010. **8**(12): p. 1371-80.
38. Fonseca, W., et al., *Lactobacillus johnsonii supplementation attenuates respiratory viral infection via metabolic reprogramming and immune cell modulation.* Mucosal Immunol, 2017. **10**(6): p. 1569-1580.
39. Saravia, J., et al., *Respiratory Syncytial Virus Disease Is Mediated by Age-Variable IL-33.* PLoS Pathog, 2015. **11**(10): p. e1005217.
40. Elion, G.B., A. Kovensky, and G.H. Hitchings, *Metabolic studies of allopurinol, an inhibitor of xanthine oxidase.* Biochem Pharmacol, 1966. **15**(7): p. 863-80.
41. Rock, K.L., H. Kataoka, and J.J. Lai, *Uric acid as a danger signal in gout and its comorbidities.* Nat Rev Rheumatol, 2013. **9**(1): p. 13-23.
42. Huff, R.D., et al., *Regulation of xanthine dehydrogensase gene expression and uric acid production in human airway epithelial cells.* PLoS One, 2017. **12**(9): p. e0184260.
43. Kool, M., et al., *An unexpected role for uric acid as an inducer of T helper 2 cell immunity to inhaled antigens and inflammatory mediator of allergic asthma.* Immunity, 2011. **34**(4): p. 527-40.
44. Hara, K., et al., *Airway uric acid is a sensor of inhaled protease allergens and initiates type 2 immune responses in respiratory mucosa.* J Immunol, 2014. **192**(9): p. 4032-42.
45. Strilchuk, L., F. Fogacci, and A.F. Cicero, *Safety and tolerability of available urate-lowering drugs: a critical review.* Expert Opin Drug Saf, 2019. **18**(4): p. 261-271.
46. Dalbeth, N., T.R. Merriman, and L.K. Stamp, *Gout.* Lancet, 2016. **388**(10055): p. 2039-2052.

641 47. Shekelle, P.G., et al., *Management of Gout: A Systematic Review in Support of an American*
642 *College of Physicians Clinical Practice Guideline.* Ann Intern Med, 2017. **166**(1): p. 37-51.
643 48. Kratzer, J.T., et al., *Evolutionary history and metabolic insights of ancient mammalian uricases.*
644 Proc Natl Acad Sci U S A, 2014. **111**(10): p. 3763-8.
645 49. Christiaansen, A.F., et al., *Altered Treg and cytokine responses in RSV-infected infants.* Pediatr
646 Res, 2016. **80**(5): p. 702-709.
647 50. Nagarkar, D.R., et al., *Airway epithelial cells activate TH2 cytokine production in mast cells*
648 *through IL-1 and thymic stromal lymphopoietin.* J Allergy Clin Immunol, 2012. **130**(1): p. 225-
649 32 e4.
650 51. Han, M., et al., *Inflammasome activation is required for human rhinovirus-induced airway*
651 *inflammation in naive and allergen-sensitized mice.* Mucosal Immunol, 2019. **12**(4): p. 958-
652 968.
653 52. Liu, W., et al., *Mechanism of TH2/TH17-predominant and neutrophilic TH2/TH17-low subtypes*
654 *of asthma.* J Allergy Clin Immunol, 2017. **139**(5): p. 1548-1558 e4.
655 53. Busse, P.J., et al., *Effect of aging on sputum inflammation and asthma control.* J Allergy Clin
656 Immunol, 2017. **139**(6): p. 1808-1818 e6.
657 54. Tan, H.T., et al., *Tight junction, mucin, and inflammasome-related molecules are differentially*
658 *expressed in eosinophilic, mixed, and neutrophilic experimental asthma in mice.* Allergy, 2019.
659 **74**(2): p. 294-307.
660 55. Swart, J.F., et al., *The efficacy and safety of interleukin-1-receptor antagonist anakinra in the*
661 *treatment of systemic juvenile idiopathic arthritis.* Expert Opin Biol Ther, 2010. **10**(12): p.
662 1743-52.
663 56. Horneff, G., et al., *Experience with etanercept, tocilizumab and interleukin-1 inhibitors in*
664 *systemic onset juvenile idiopathic arthritis patients from the BIKER registry.* Arthritis Res Ther,
665 2017. **19**(1): p. 256.
666 57. Tarp, S., et al., *Efficacy and safety of biological agents for systemic juvenile idiopathic arthritis:*
667 *a systematic review and meta-analysis of randomized trials.* Rheumatology (Oxford), 2016.
668 **55**(4): p. 669-79.

58. Bettiol, A., et al., *Unveiling the Efficacy, Safety, and Tolerability of Anti-Interleukin-1 Treatment in Monogenic and Multifactorial Autoinflammatory Diseases.* Int J Mol Sci, 2019. **20**(8).
59. Gabay, C., C. Lamacchia, and G. Palmer, *IL-1 pathways in inflammation and human diseases.* Nat Rev Rheumatol, 2010. **6**(4): p. 232-41.
60. Kullenberg, T., et al., *Long-term safety profile of anakinra in patients with severe cryopyrin-associated periodic syndromes.* Rheumatology (Oxford), 2016. **55**(8): p. 1499-506.
61. Gattorno, M., et al., *Persistent efficacy of anakinra in patients with tumor necrosis factor receptor-associated periodic syndrome.* Arthritis Rheum, 2008. **58**(5): p. 1516-20.
62. Desch, A.N., et al., *CD103+ pulmonary dendritic cells preferentially acquire and present apoptotic cell-associated antigen.* J Exp Med, 2011. **208**(9): p. 1789-97.
63. Helft, J., et al., *Cross-presenting CD103+ dendritic cells are protected from influenza virus infection.* J Clin Invest, 2012. **122**(11): p. 4037-47.
64. Martinez-Gonzalez, I., et al., *ILC2 memory: Recollection of previous activation.* Immunol Rev, 2018. **283**(1): p. 41-53.
65. Ackerson, B., et al., *Severe Morbidity and Mortality Associated With Respiratory Syncytial Virus Versus Influenza Infection in Hospitalized Older Adults.* Clin Infect Dis, 2019. **69**(2): p. 197-203.
66. Kwon, Y.S., et al., *Risk of mortality associated with respiratory syncytial virus and influenza infection in adults.* BMC Infect Dis, 2017. **17**(1): p. 785.
67. Falsey, A.R., et al., *Respiratory syncytial virus infection in elderly and high-risk adults.* N Engl J Med, 2005. **352**(17): p. 1749-59.

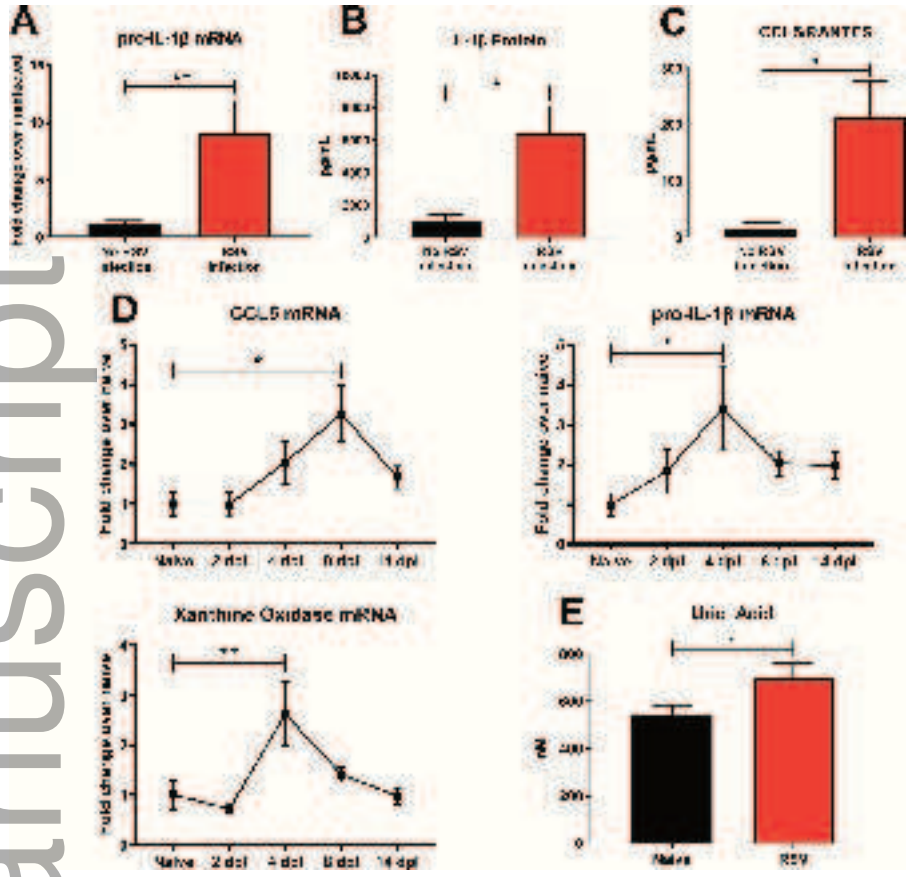

all_14310_f1.tif

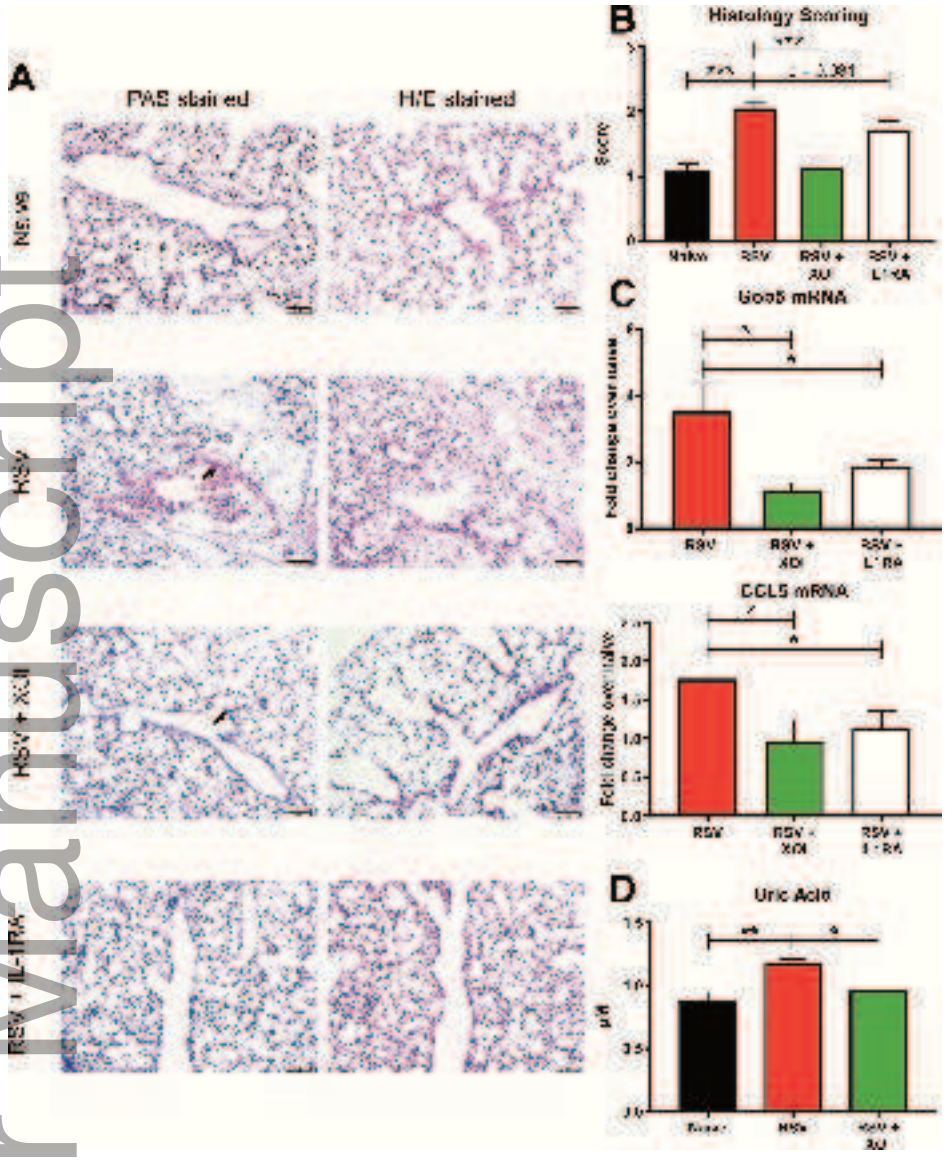

all_14310_f2.tif

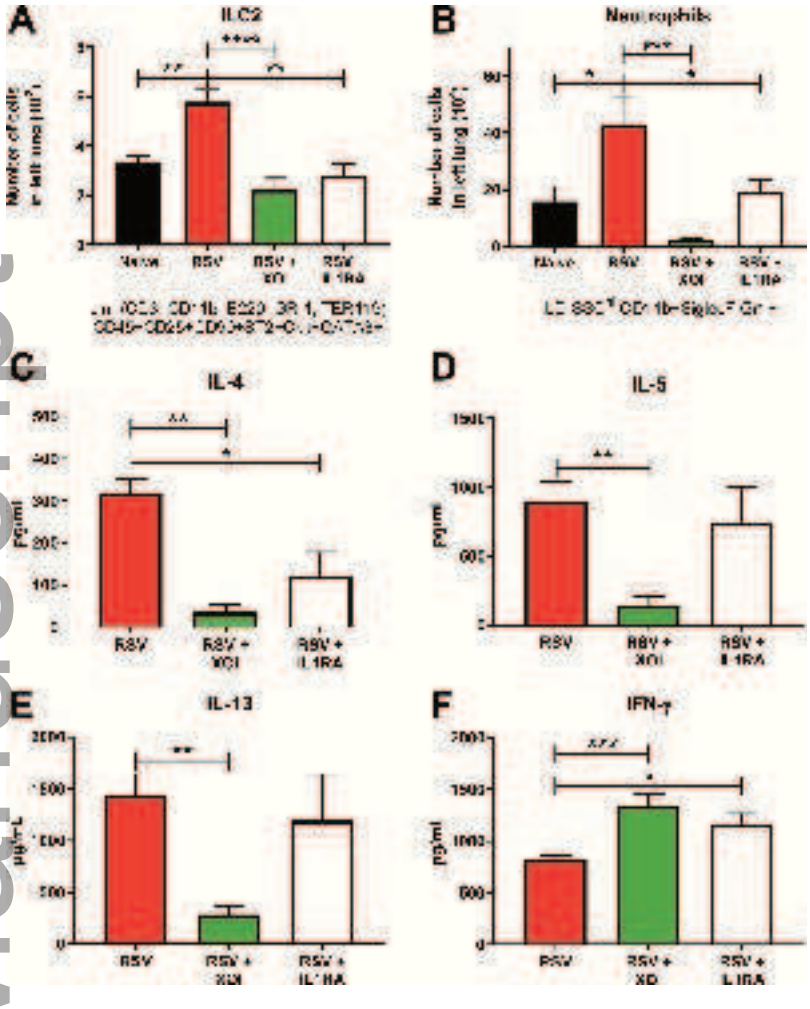

all_14310_f3.tif

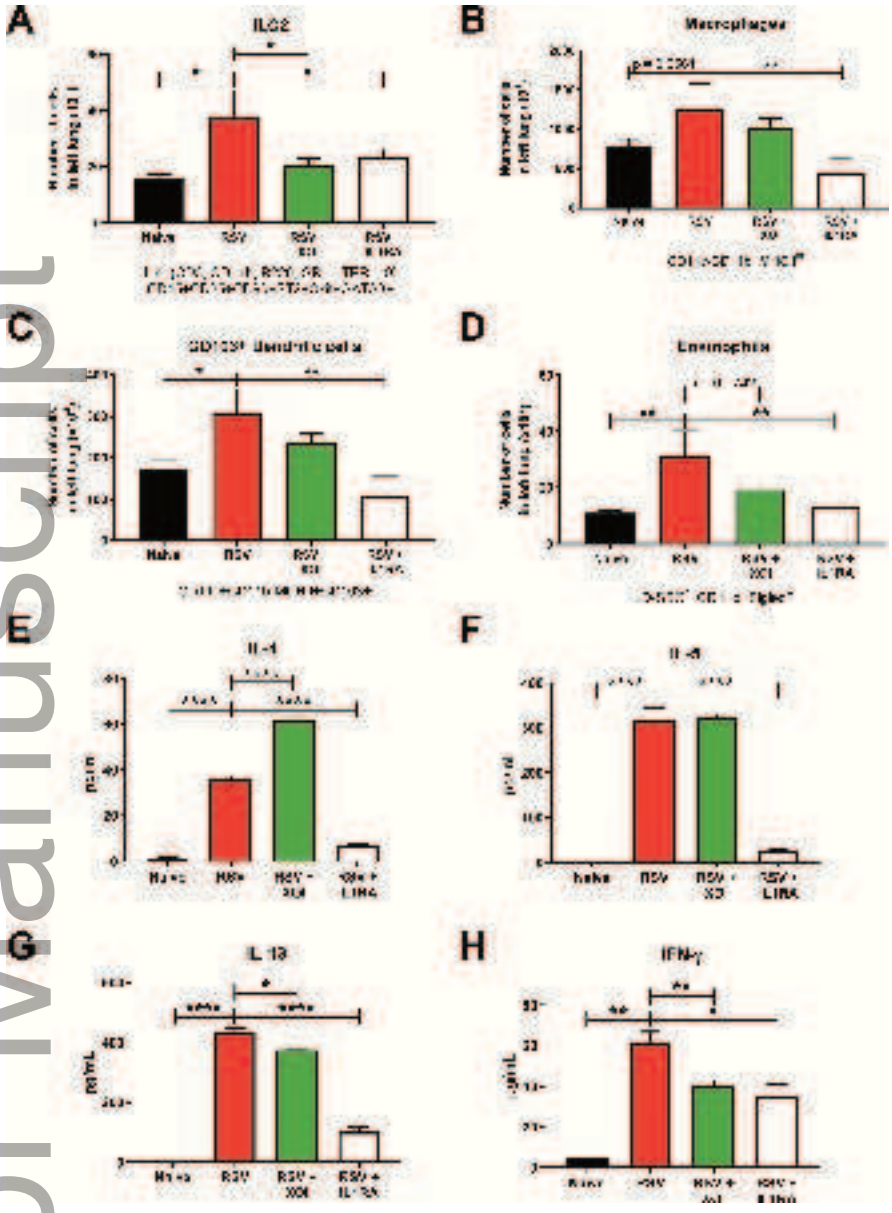

all_14310_f4.tif

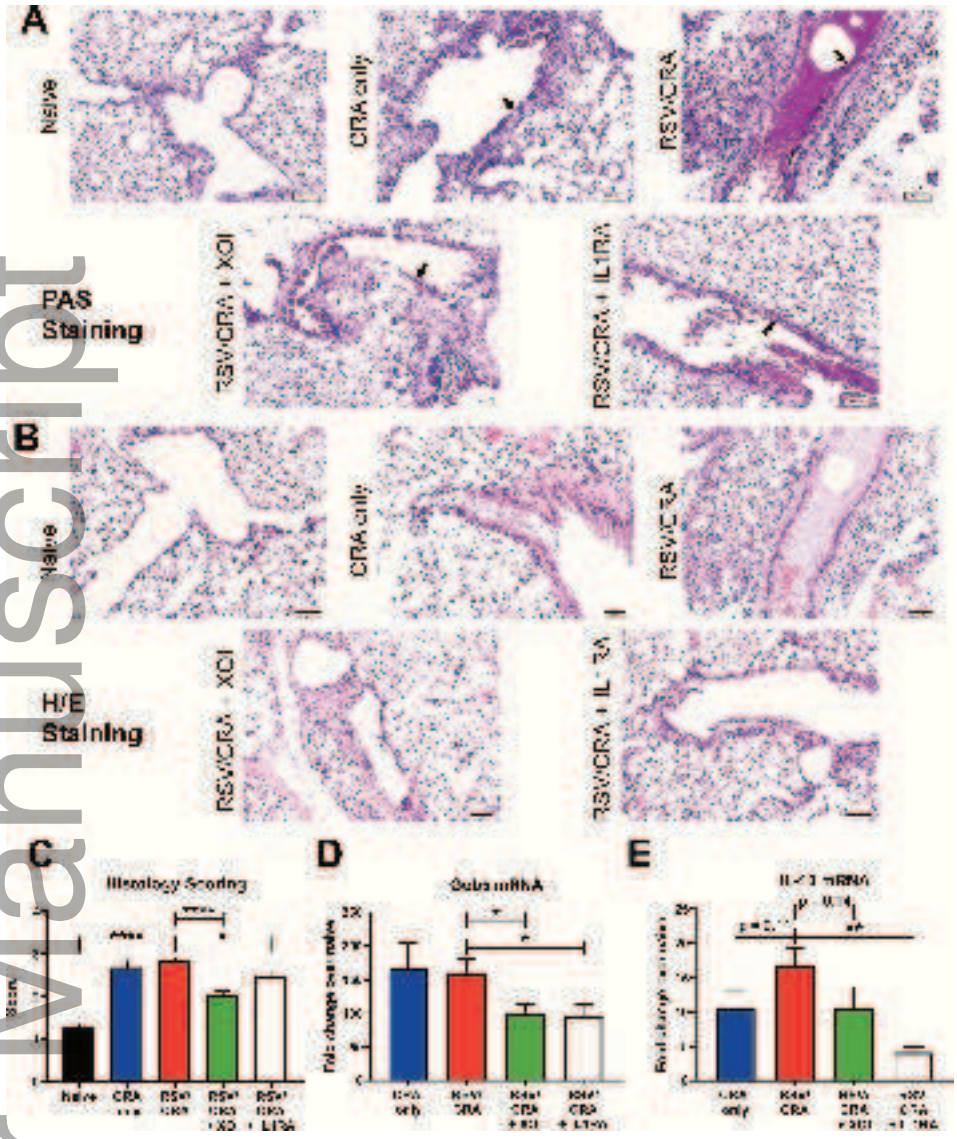

all_14310_f5.tif

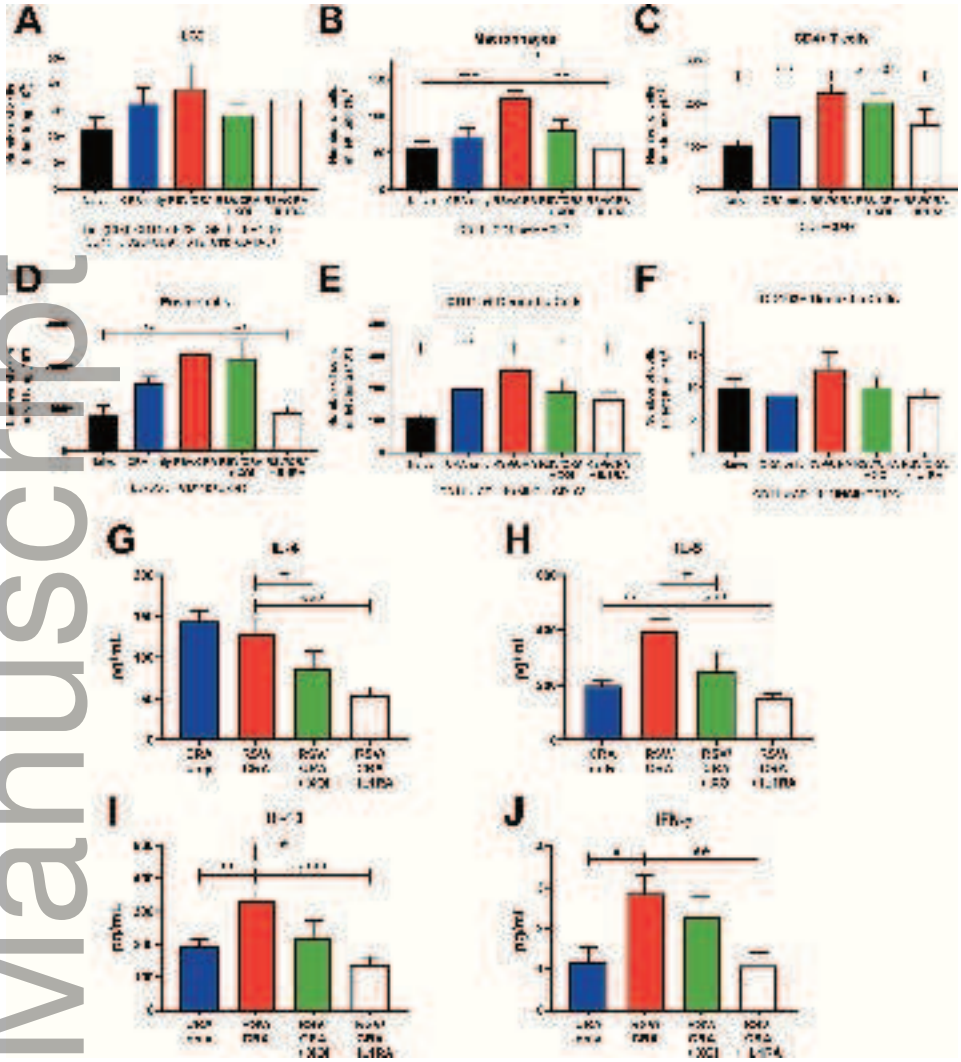

all_14310_f6.tif